Lab on a Chip

RSC Publishing

PAPER

View Article Online
View Journal | View Issue

Cite this: *Lab Chip*, 2013, **13**, 4451

A CMOS wireless biomolecular sensing system-on-chip based on polysilicon nanowire technology†

C.-W. Huang,[a] Y.-J. Huang,[a] P.-W. Yen,[b] H.-H. Tsai,[c] H.-H. Liao,[c] Y.-Z. Juang,[c] S.-S. Lu*[a] and C.-T. Lin*[abd]

Received 4th July 2013,
Accepted 4th September 2013

DOI: 10.1039/c3lc50798j

www.rsc.org/loc

As developments of modern societies, an on-field and personalized diagnosis has become important for disease prevention and proper treatment. To address this need, in this work, a polysilicon nanowire (poly-Si NW) based biosensor system-on-chip (bio-SSoC) is designed and fabricated by a 0.35 μm 2-Poly-4-Metal (2P4M) complementary metal-oxide-semiconductor (CMOS) process provided by a commercialized semiconductor foundry. Because of the advantages of CMOS system-on-chip (SoC) technologies, the poly-Si NW biosensor is integrated with a chopper differential-difference amplifier (DDA) based analog-front-end (AFE), a successive approximation analog-to-digital converter (SAR ADC), and a microcontroller to have better sensing capabilities than a traditional Si NW discrete measuring system. In addition, an on–off key (OOK) wireless transceiver is also integrated to form a wireless bio-SSoC technology. This is pioneering work to harness the momentum of CMOS integrated technology into emerging bio-diagnosis technologies. This integrated technology is experimentally examined to have a label-free and low-concentration biomolecular detection for both Hepatitis B Virus DNA (10 fM) and cardiac troponin I protein (3.2 pM). Based on this work, the implemented wireless bio-SSoC has demonstrated a good biomolecular sensing characteristic and a potential for low-cost and mobile applications. As a consequence, this developed technology can be a promising candidate for on-field and personalized applications in biomedical diagnosis.

Introduction

Because of aging problems in modern society, the healthcare system has encountered a paradigm shift in bio-diagnosis technologies.[1] The traditional, established methods in clinical biomolecular diagnosis are polymerase chain reaction (PCR) for nucleic acids and enzyme linked immunosorbent assay (ELISA) for proteins. These clinical standard methods are designed for well trained technicians and well equipped laboratories. In other words, they are time consuming and cost-ineffective. Because of changes in society infrastructure, however, there is an increasing demand for a real-time and low-cost biomolecular diagnosis techniques to promote healthcare paradigm shifts, *e.g.* personalized medicine. To match this unmet need, a point-of-care testing (POCT) system has been preposed and developed by researchers.[2] Ideally, a POCT system should have characteristics of low cost, high portability, simple operational process, and analytical diagnosis. To accomplish these characteristics, lab-on-chip (LOC) technologies are essential toward developments of POCT because of their advantages, *e.g.* small-size, quick-response, and mobile capabilities.[3] Since most of LOC are based on mature nano/micro fabrications, it is intriguing to harness the momentum from CMOS technologies. As a consequence, CMOS compatible biosensing devices, *e.g.* microcantilevers,[4–7] ion-sensitive field-effect-transistors (ISFET),[8–9] and nanowires (NW),[10–13] have been intensively investigated. Among these CMOS compatible biosensing devices, the nanowire biosensing technique is a promising candidate because of its high sensitivity and fast response.[14,15]

Because the potential of the nanowire biosensing technique, its design and implementation have been proposed and examined. For instance, Patolsky *et al.* fabricated a single crystal silicon (SCS) NW by chemical vapor deposition (CVD) and examined its good biosensing capabilities.[16] However, this technique suffers from a low yield rate because of device arrangements. On the other hand, Ivanov *et al*. fabricated a SCS NW by using electron beam (e-beam) lithography with silicon-on-insulator (SOI) substrates.[17] But SOI wafer and e-beam lithography are not cost-effective, as a consequence, a SCS NW implemented by this method is limited within research demonstrations. Furthermore, Lin *et al.* demonstrates

[a] *Graduate Institute of Electronics Engineering, National Taiwan University, Taipei 10617, Taiwan. E-mail: sslu@cc.ee.ntu.edu.tw*

[b] *Graduate Institute of Biomedical Electronics and Bioinformatics, National Taiwan University, Taipei 10617, Taiwan*

[c] *National Chip Implementation Center, National Applied Research Laboratories, Hsinchu 30075, Taiwan*

[d] *Department of Electrical Engineering, National Taiwan University, Taipei 10617, Taiwan. E-mail: timlin@cc.ee.ntu.edu.tw; Fax: +886 2 2368 1679; Tel: +886 2 3366 9603*

† Electronic supplementary information (ESI) available. See DOI: 10.1039/c3lc50798j

that a poly-crystalline silicon (poly-Si) NW fabricated by a sidewall spacer technique has good biosensing responses.[18] Although this technique shows a low-cost method towards NW biosensing technology, the reliability and uniformity issues of its etching process impede this sidewall poly-Si NW technique. In addition, complicated measurement setups of these developed NW biosensing devices also limit them within research laboratory environments. To accomplish requirements of POCT based on NW biosensing technologies, it is necessary to demonstrate a method with low-cost manufacturing, high-reliability fabrication, and ease of usage for field applications.

In this paper, we report a poly-Si NW based biosensor system-on-chip (bio-SSoC) which was implemented by the commercially available 0.35 μm 2P4M standard CMOS process. With a simple post-etching process, a label-free bio-SSoC with high sensitivity and real-time detection can be realized. The bio-SSoC has integrated with a chopper DDA-based AFE, a SAR ADC, a micro controller and an OOK wireless acquisition circuit to promote its sensing quality and remote detection capability. In other words, this work not only demonstrates the potential of mobile biomolecular diagnosis for on-field testing but also paves the way toward individual diagnosis for personalized healthcare. For the first time, a standard CMOS technology has been bridged with a nanowire bio-diagnosis technique. The mature CMOS technology enhances productivity and ease of operation for biomedical applications. On the other hand, the emerging micro-bio-diagnosis applications also promote the value of CMOS integrated systems.

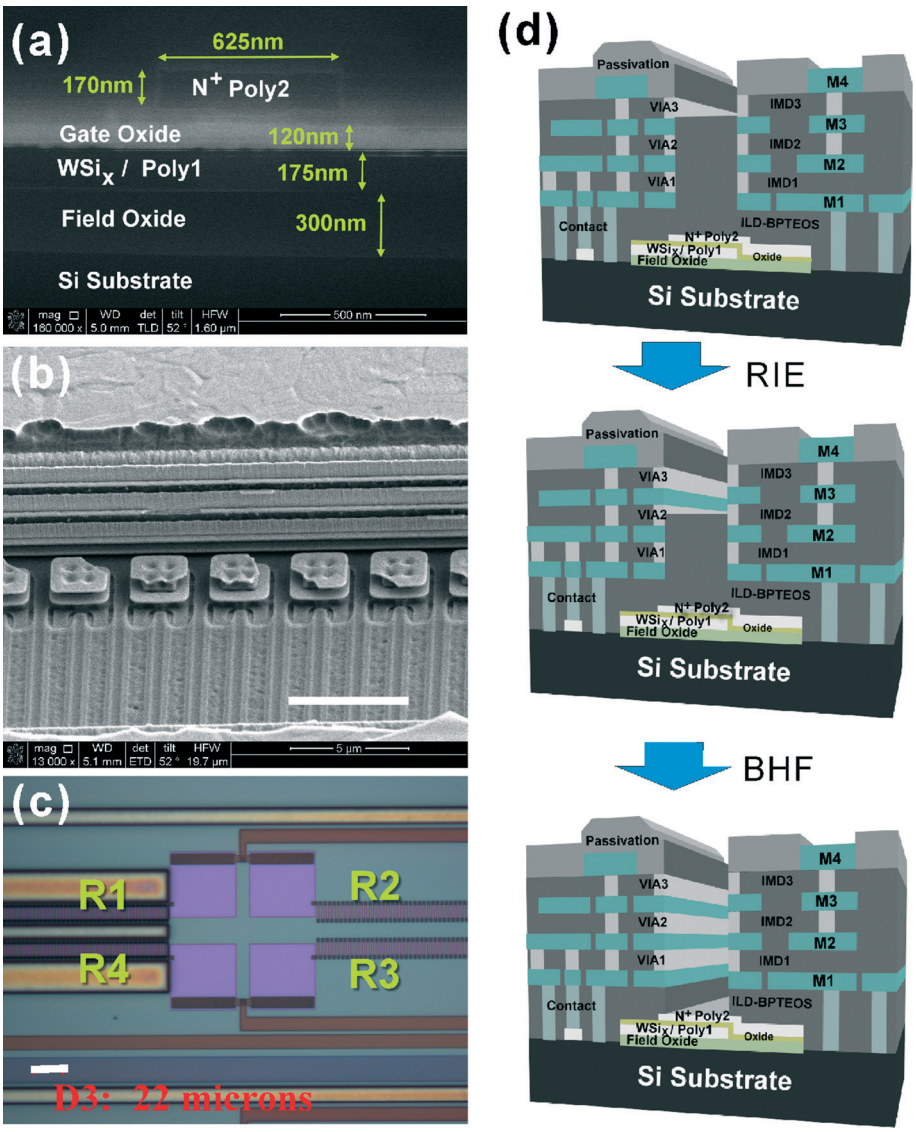

Fig. 1 (a) A cross-section SEM image of fabricated poly-Si NW sensing device. The cross-section is generated by FIB. (b) A SEM image of fabricated poly-Si NW in meander form (white bar represents 5 μm). (c) An optical image of fabricated poly-Si NW in Wheatstone bridge (white bar represents 22 μm). (d) A schematic of the post-etching process to remove TEOS oxide on the top of the poly-Si NW sensing device.

Materials and methods

Design and fabrication of poly-Si NW biosensor

To achieve low-cost and standardized characteristics, a 0.35 μm 2P4M commercially-available CMOS fabrication process is adopted to monolithically implement the poly-Si NW with circuit systems. In this process, there are two poly-silicon layers. The poly1 layer is designed for a gate material, *i.e.* degenerated doping poly-silicon. On the other hand, the N^+ poly2 layer is designed for on-chip capacitors, *i.e.* lower doping of N^+ poly2 (sheet resistance: 50 ohms per square) than that of poly1 layer. Based on previous studies,[19–20] the biomolecular sensitivity can be enhanced by low-doping semiconductor-based NW. Therefore, poly-Si NW biosensors are designed to use N^+ poly2 layer. The cross section of a fabricated poly-Si NW biosensor can be shown in Fig. 1(a). To have a good design window of interface circuits, *e.g.* an adequate output impedance of a sensor, the meander shape of poly-Si NW shown as Fig. 1(b) is employed to obtain higher resistance suitable for interface circuits. Since the conductance of poly-Si NW is the quantity to be measured, a classical sensor arrangement, *i.e.* a Wheatstone bridge architecture, is used to improve not only sensitivity but also the common-mode rejection ratio (CMRR). Fig. 1(c) shows the optical image of a set of fabricated Wheatstone-bridged poly-Si NW biosensors. In addition, a special layout of metal layers is used to minimize the poly-Si NW biosensor region and protect other on-chip circuits. In this design, metal1/VIA1, metal2/VIA2, metal3/VIA3, and metal4 are stacked around poly-Si NW biosensors, shown as Fig. 1(d). This structure forms an etching stop sidewall to prevent lateral etching during a post-etching process. This is important to enhance the yield rate of the post-etching process.

To functionalize poly-Si NW biosensors after the standard CMOS process, a post-etching process is necessary to reduce the thickness of oxide layers, TEOS oxide layers, deposited on the top of biosensors. To reduce the complexity of the post-etching process, it should be noted that the passivation layer, Si_3N_4, is removed by using a standard CMOS process, *i.e.* PAD layer design. The PAD layer is originally designed to open the passivation layer to form contact pads in metal4. After opening the passivation layer, two steps of dielectric etching, TEOS oxide etching, are necessary. The first step is reactive ion etching (RIE) by using trifluoromethane (CHF_3) process gas. Since long-time RIE may cause charging damages to both poly-Si NW and on-chip circuits, wet etching with buffered hydrofluoric acid (BHF) is used as the second-etching step to further reduce oxide thickness to 100 nm. Because N^+ poly2 is doped to have a limited resistance, this oxide on the top of poly-Si NW is essential to reduce the leakage current through the solid/liquid interface between poly-Si and the aqueous environment.[21] It is critical to improve the signal-to-noise ratio (*S*/*N* ratio) of fabricated biosensing devices. The etching process can be seen in Fig. 1(d).

Architecture design of on-chip sensors and circuits

To increase the biomolecular sensitivity of a semiconductor NW biosensor, based on previous works,[19–20] a low-doping, small-diameter, and thin-thickness NW is preferred. However, all of these parameters are restricted by the CMOS manufacturer. As a consequence, an adequate sensor-circuit co-design is important to obtain a good performance biosensor system-on-chip. For poly-Si NW biosensors, as aforementioned, a Wheatstone bridge architecture is used. In this arrangement, a full-bridge mode is used to minimize variations from testing environments and fabrication processes. Compared with other kinds of sensor arrangements, moreover, the full-bridge Wheatstone bridge can double the output differential signal. In addition to poly-Si NW biosensors, an on-chip junction-based CMOS temperature sensor is also designed to offer the temperature calibration capability for biomolecular sensing applications. To reduce complexity and power consumption, the temperature sensor shares the same signal path with poly-Si NW biosensors by a multiplexer control.

Fig. 2(a) shows the schematic architecture of a poly-Si NW sensor arrangement. Based on the full-bridge setup, two poly-Si NWs (R1 and R4) are exposed by the post-etching process and the other two poly-Si NWs (R2 and R3) are still covered by dielectric (oxide) and passivation (nitride) layers. As a consequence, only R1 and R4 are functionalized by the probe ssDNA. Since the poly-Si NW is N-type doping and DNA is negative charged in PBS environment, the electron carriers within poly-Si NWs are repelled from the NW surface as the target ssDNA hybridizing with probe ssDNA. Therefore, this specific hybridization phenomena leads to lowering conductance of the exposed poly-Si NW sensing devices, *i.e.* increasing the resistance of R1 and R4. In other words, the complementary target ssDNA with specific binding affinity to the HBV probe ssDNA can be expected to induce lower conductance, *i.e.* higher resistance, of the poly-Si NW than that of other non-complementary ssDNAs. As a consequence, the increase of R1 and R4 results in the decrease in the Wheatstone bridge output voltage, *i.e.* $I_A V_{in}^+ - I_A V_{in}^-$. This voltage is amplified by DDA AFE for further signal processes. It should be noted that the amplified gain can be adjusted from 1 X to 40 X by using different external resistors.

To condition the Wheatstone bridged poly-Si NW biosensors, a chopper DDA based AFE is designed to obtain the amplified differential voltage signal. The DDA architecture has been demonstrated to improve detection quality by offering characteristics of low-noise, high CMRR, and rail-to-rail input range. The functionality of the designed DDA AFE was demonstrated by our previous work.[22] To convert the amplified analog signal to a built-in digital signal processor, a 10-bit SAR ADC is used because of its low-power consumption characteristic. To integrate the portability of the developed biosensing system-on-chip, furthermore, the major function of the built-in processor is packing digitized

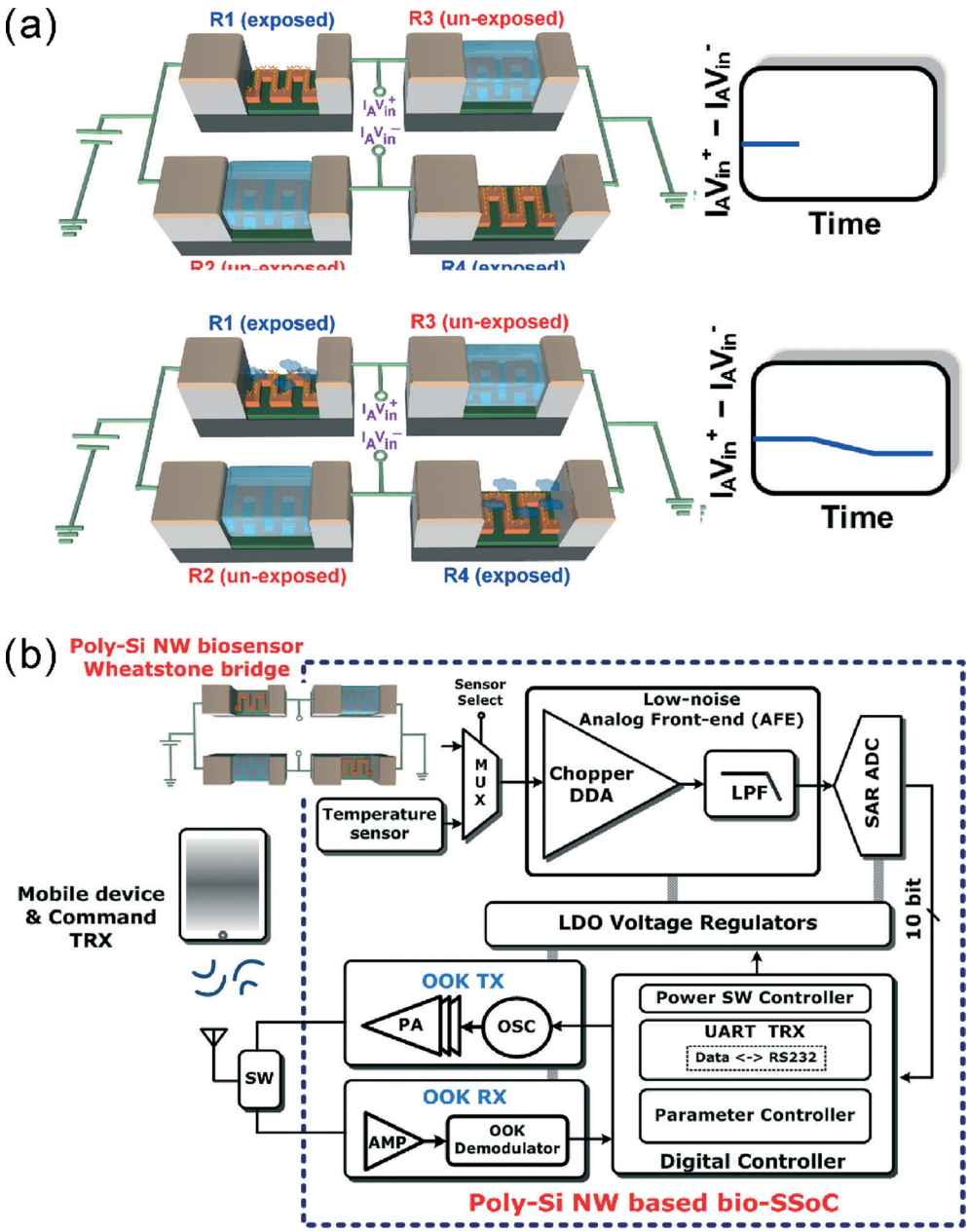

Fig. 2 (a) A schematic of the Wheatstone bridge architecture composed of four poly-Si NWs. As target ssDNA attached, the resistance of the exposed poly-Si NW increases and the output voltage of the Wheatstone bridge decreases. (b) A system architecture of the developed bio-SSoC. The input, *e.g.* poly-Si NW or temperature sensor, of AFE can be chosen by a multiplexer (MUX) through a microcontroller digital output. This offers a real-time temperature monitoring and calibration capability for poly-Si NW measurement.

signals into a RS232 format. Then the packed signal can be transmitted by a built-in OOK wireless transceiver (TX/RX) to external devices, *e.g.* mobile platforms, for further recording and analysis. Based on this system architecture, both data transmission and command receiving can also be implemented to realize the mobile capability. The whole system architecture is shown in Fig. 2(b).

Experimental protocols and setups

Since functionalized and experimental processes are in aqueous environments, the passivation of the fabricated bio-SSoC is necessary to protect the on-chip circuits from damages. Moreover, bonding wires also need to be passivated to avoid short-circuit to ionic buffers. To achieve this passivation after the bio-SSoC wire is bonded on a designed printed-circuit-board (PCB), epoxy is used to cover the bonding pads on the PCB, PADs on the bio-SSoC, and bonding wires. To retain aqueous samples on the top of bio-SSoC, in addition, a plastic reservoir is mounted on the PCB board and encloses the whole bio-SSoC with bonding wires. Then all the bio-related experimental protocols are processed within the constructed reservoir.

To examine the biomolecular sensing capability of the developed poly-Si NW based sensing device, a 19 mers probe single-strained deoxyribonucleic acid (ssDNA) with the sequence 5'-SH-CCGATCCATACTGCGGAAC-3' (Genomics BioSci & Tech, Taiwan) is used. This probe ssDNA sequence is chosen because it is the highly conservative region for all genotypes of the Hepatitis B Virus (HBV).[23] This sequence is also the standard HBV probe DNA in clinical examinations, *e.g.* polymer chain reaction (PCR). To functionalize the fabricated poly-Si NW sensing device, the surface modification is necessary. The modification protocol can be briefly described as: (1) 2% ethanol solution with 3-aminopropyltriethoxysilane (APTES, Sigma-Aldrich) is injected for 30 minutes to form a monolayer on the surface of the exposed silicon dioxide on the top of poly-Si NW; (2) after washing with ethanol solution several times to remove unreacted APTES, the device is dried by nitrogen gas and baked at 120 °C for 10 minutes to remove the residual ethanol; (3) 4 mM sulfosuccinimidyl-4-(*N*-maleimidomethyl)cyclohexane-1-carboxylate (sulfo-SMCC, Sigma-Aldrich) is injected for one hour to interact with the amine group of ATPES to form a maleimide-activated functional group; (4) after washing with deionized water (DI) several times to remove the non-reacted sulfo-SMCC, 10 μM thiol-modified 19 mers probe HBV ssDNA with phosphate buffered saline buffer (PBS, UniRegion Bio-Tech) is injected for one hour; (5) the device is washed by DI water several times to remove the non-specific binding probe ssDNA and is ready for testing. To examine the sensitivity and selectivity of the developed bio-SSoC, on the other hand, the experimental protocol can be briefly described as: (1) inject PBS buffer for 90 seconds and measure the device output voltage to be the base line; (2) remove PBS buffer and inject specific concentration of testing target ssDNAs, *i.e.* complementary and non-complementary HBV DNA sequence, in PBS buffer for a 90-second incubation; (3) wash the reservoir with PBS buffer with a four fold volume to sample volume to remove un-hybridized target ssDNAs and wait 5 minutes for a steady state of the sensor output; (4) measure the sensor output voltage in the PBS buffer environment.

To visualize the fabricated chip, a scanning electron microscope (SEM, ERA-8800, ELIONIX Inc., Japan) and a focused ion beam (FIB, Nova 600 NanoLab, FEI Company, USA) are used to obtain top and cross-section views of the fabricated bio-SSoC. To characterize the poly-Si NW sensing device, on the other hand, the output voltage from AFE is recorded by a source-meter (Keithley 2400, USA). Finally, the whole wireless bio-SSoC is performed with a 433 MHz transceiver connected to a personal computer through RS232 and recorded by LabVIEW (National Instruments, USA).

Results and discussion

Characterization of temperature sensor and AFE

The fabricated poly-Si NW bio-SSoC has a chip area with 2.5 mm by 2.5 mm. As described above, the SSoC chip includes functional blocks of poly-Si NW sensors, DDA AFE, SAR ADC, a microcontroller, and a OOK transceiver as shown in Fig. 3(a). To examine the function of AFE on the fabricated bio-SSoC, the built-in on-chip junction-based CMOS temperature sensor is used as an input signal of the DDA AFE. Utilizing an oven to control the environmental temperature, the on-chip temperature sensor is characterized (shown in Fig. S1†). While a circuit bias point (V_{REF}) remains nearly constant, it is clear that the temperature sensor output voltage has a linear response with the temperature variation. Based on this experiment, in addition, AFE also shows a stable performance with the temperature variation. To understand the chip functionality under an aqueous buffer environment, furthermore, a bio-SSoC is tested with a plastic reservoir filled with PBS buffer solution as operated under bio-related experiments. The measured temperature while all circuit blocks are functional for 20 minutes. The temperature variation is within 1 °C and could result from environmental conditions (shown as Fig. S2†).

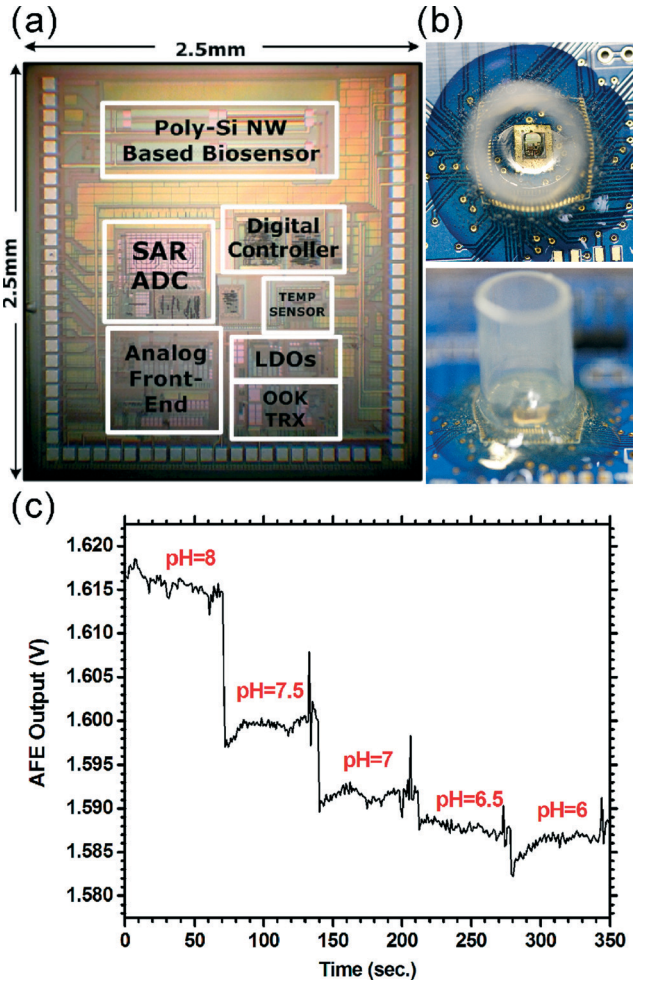

Fig. 3 (a) An image of the fabricated bio-SSoC. In this image, regions of functional blocks are labeled. After post-etching, the bio-SSoC is wire-bonded on a PCB board and enclosed by a plastic reservoir with epoxy. (b) Images of the set-up bio-SSoC with a plastic reservoir for further bio-related testing. (c) An experimental result of pH measurement by the poly-Si NW sensing device.

Validation of poly-Si NW sensing devices

To verify the functionality of the fabricated poly-Si NW sensor, a typical ion-sensitivity test, *i.e.* response to pH variations, is preformed. The test is carried at the aforementioned experimental reservoir as shown in Fig. 3(b). Since the poly-Si NW is n-type, its conductance decreases with increasing pH due to the decrease of protonations on the poly-Si NW surface. Fig. 3(c) shows a real-time experimental result of a pH testing. In this experiment, the poly-Si NW sensor has a better response at basic conditions, *i.e.* pH $>$ 7, than that at acid conditions, *i.e.* pH $<$ 7. Stern *et al.* demonstrate similar behaviour of *n*-type In_2O_3 NW.[24] As a consequence, the functionality of the *n*-type poly-Si NW sensor can be justified. Furthermore, the validation of the post-etching process can also be examined (shown as Fig. S3†). Under the same peripheral setup, the sensor response is larger with post-etching (0.23% per decay) than that without post-etching (0.051% per decay). In addition, the limit-of-detection (LOD) of the device with and without post-etching are 10 fM and 10 pM, respectively. Therefore, the post-etching process is necessary to obtain good sensing characteristics.

Characterization of poly-Si NW sensing devices

The poly-Si NW biosensor sensitivity to HBV target ssDNA can be demonstrated as Fig. 4(a). Following the experimental protocol described above, the voltage output from DDA AFE was directly measured and recorded by a Keithley sourcemeter. Although both doping effect and polycrystalline structure deteriorate the sensing performance of the fabricated poly-Si NW sensor, based on the experimental result, a distinguishable voltage output can be measured with a limit-of-detection (LOD) at 10 fM in PBS buffer environments. This outstanding sensing capability could be caused by three factors: (1) Large sensing region: the fabricated poly-Si NW sensing device is in meander form with 625 nm width and 2.5 mm length. While keeping the width small, the small width/length ratio (W/L) increases the hybridization probability of HBV target ssDNAs. (2) Sample injection by drop into the

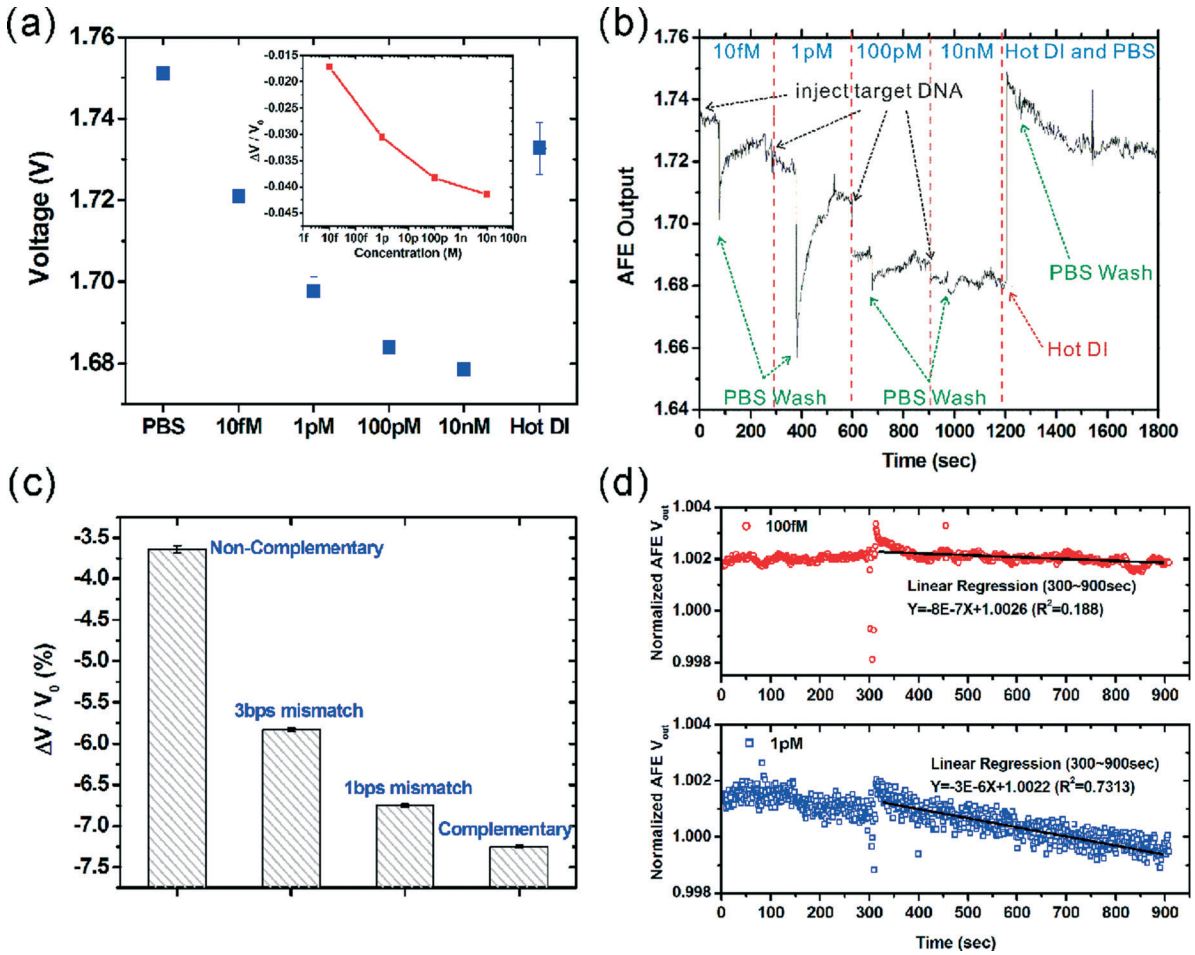

Fig. 4 (a) An experimental HBV DNA sensitivity test of the developed bio-SSoC (N = 3). After washing with hot DI water, the sensor readout was recovered. This shows the output voltage variation is due to the binding of HBV DNA. (b) A time history of a HBV DNA sensitivity test. It should be noted that the measurement was obtained after washing with PBS buffer. (c) An experimental HBV DNA selectivity test of the developed bio-SSoC (N = 3). (d) An experimental time history of HBV DNA binding test under different concentrations. In this experiment, the measurement was continuously monitored for more than 10 minutes without washing with PBS buffer. The higher concentration of target HBV DNAs leads to a higher binding rate and results in a steeper slope.

reservoir: the injection of aqueous samples/buffers is done by micro-pipette dropping. The drop generates a convectional flow within the reservoir. As a consequence, target ssDNAs approach to the surface of poly-Si NW sensor by not only diffusion but also convection. (3) On-chip signal condition: the on-chip signal amplification of DDA AFE enhances the signal-to-noise ratio. On the other hand, Fig. 4(b) shows a real-time sensor response as an injection of different concentration of target ssDNAs and wash by PBS buffer. At the end of the experiment, hot DI water was injected into the reservoir for 90 seconds to de-hybridize the target ssDNAs. After re-injecting PBS buffer to replace hot DI water, the measured output voltage is similar to the read-out voltage of 10 fM. This shows the sequential voltage variation is resulting from the hybridization of different concentration of target ssDNAs. It should be noted that the read-out voltage can not be back to the initial measurement of PBS buffer because of the nonspecific binding effect.

Due to associations between genotype and mutants of HBV and Hepatocellular Carcinoma (HCC), the selectivity is also critical in clinical applications. Following the same experimental protocols as the sensitivity test, the selectivity of the developed poly-Si NW biosensor is examined by using different kinds of testing ssDNAs, *i.e.* complementary: 5'-GTTCCGCAGTATGGATCGG-3'; one base-pair (1 bps) mismatch: 5'-GTTCCGTAGTATGGATCGG-3'; three base-pair (3 bps) mismatch: 5'-GTTCCGTGATATGGATCGG-3'; and non-complementary sequence: 5'-ACCTTATCTACCTACCTAT-3'. In the selectivity test, the testing concentration is 1 μM for all kinds of testing ssDNAs and the amplified gain is also adjusted to accommodate this highly concentrated condition. Fig. 4(c) shows the selectivity experimental result. Since the binding affinity of DNA is dependent on the number of matching pairs, the experimental result demonstrates that the sensor response is different according to different kinds of testing ssDNAs. While non-complementary testing ssDNAs has 3.65% output voltage change because of the non-specific binding under such a concentrated condition, there is 0.5% output-voltage difference between 1 bps mismatch and complementary testing ssDNAs. According to this experimental result, the developed poly-Si NW biosensor has the capability to distinguish 1 bps mismatch from complementary testing ssDNAs.

Instead of washing away un-bound ssDNA samples by PBS to measure the device response in a standard environment, the binding process can be estimated as ssDNA samples stay within the experimental reservoir during a period of time. Fig. 4(d) shows the developed poly-Si NW sensor responses to target ssDNA samples with different concentrations. In Fig. 4(d), the experimental slopes are -8×10^{-7} and -3×10^{-6} for 100 fM and 1 pM, respectively. Since the binding per unit time of target ssDNAs is more in high concentrations than that in low concentrations, these slopes implicitly indicate the concentration difference of target ssDNA samples.

Examination of wireless bio-SSoC

As aforementioned, the integration of a microcontroller with a wireless transceiver enables the portability of the developed bio-SSoC. To realize the wireless communication between a personal computer and a bio-SSoC, as shown in Fig. 5(a), an off-the-shelf 433 MHz antenna module is used to transmit digital data. On the other hand, another 433 MHz transceiver chip with an antenna is used to receive the data and pass the data to a personal computer by RS232. Fig. 5(a) shows the result of sensitivity measurements through a fully functional bio-SSoC. The output of this experimental result keeps its digital format to demonstrate the original data received by RS232 at the personal computer. On the other hand, cardiac troponin I protein (cTnI) is also experimentally tested to demonstrate the biomolecular diagnosis capability of the developed bio-SSoC as shown in Fig. 5(b). The experimental protocol of cTnI testing is similar to HBV ssDNA except there

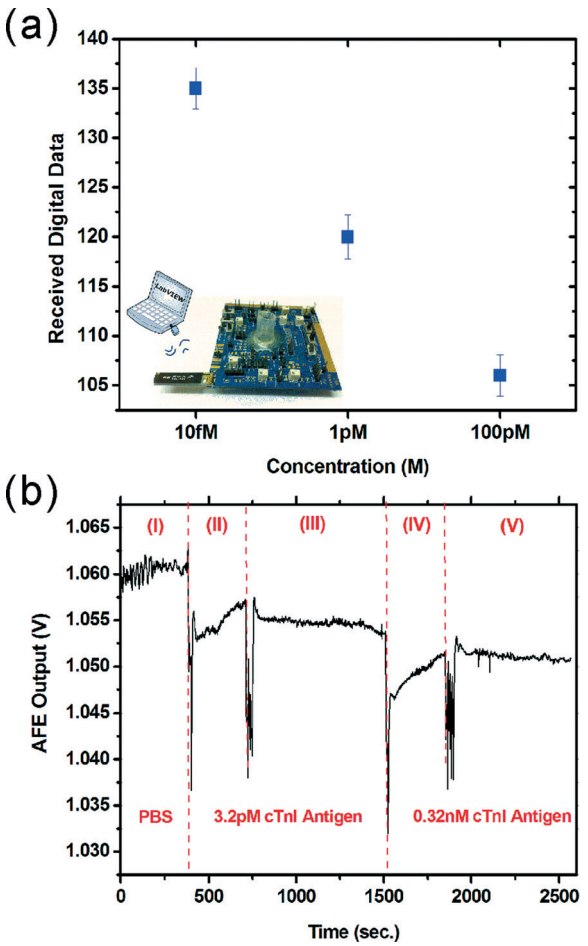

Fig. 5 (a) A experimental demonstration of a functional wireless bio-SSoC for HBV DNA detection. The small image shows the wireless setup of this experiment. (b) An experimental time history of cTnI detection. Region (I) represents the response of pure PBS buffer. At Region (II), 3.2 pM cTnI sample was injected into the testing reservoir. At Region (III), pure PBS buffer was used to wash away un-bound cTnI antigen. At Region (IV) and Region (V), the same experimental protocol was repeated for measuring the 0.32 nM cTnI sample.

Table 1 Comparison table of nanowire based biosensor for ssDNA and cTnI

Fabrication process	Materials	Analytes	LOD	Ref.
E-beam Lithography	SOI	ssDNA	25 pM	25
Chemical Vapor Deposition	Single-crystalline silicon	ssDNA	10 pM	26
DUV lithography	SOI	ssDNA	10 fM	27
Chemical Vapor Deposition	Single-crystalline silicon	ssDNA	10 fM	28
TSMC 0.35 μm CMOS process	***Poly-crystalline silicon***	***ssDNA***	***10 fM***	***This work***
Physical Vapor Deposition	SnO_2	cTnI	2 ng ml^{-1}	29
Electrochemical Deposition	Polyaniline	cTnI	250 fg ml^{-1}	30
Stepper Lithography	SOI	cTnI	~92 pg ml^{-1}	31
Current Clinical Method	ELISA	cTnI (in whole-blood)	0.14 ng ml^{-1}	32
TSMC 0.35 μm CMOS process	***Poly-crystalline silicon***	***cTnI***	***3.2 pM***	***This work***

is a longer incubation time for cTnI. The demonstrated stable detection range is from 3.2 pM to 320 pM as measuring in PBS environments. These experimental results show the potential of the developed SSoC to be employed in various applications. Furthermore, the comparison between previous works and the developed bio-SSoC can be shown in Table 1.

Conclusions

This paper presents a fully integrated bio-SSoC for HBV ssDNA detection based on poly-Si NW sensing devices. The bio-SSoC is fabricated by a 0.35 μm 2-Poly-4-Metal complementary metal-oxide-semiconductor (CMOS) process provided by a commercial semiconductor foundry. Utilizing a special *via* design, the post-etching process is able to remove covered oxide without affecting surrounded CMOS circuits. These on-chip interface circuits improve the signal from poly-Si NW sensing devices. On the other hand, a built-in temperature sensor indicates that the temperature remains steady while the bio-SSoC is operating. As a consequence, a LOD of 10 fM can be achieved and 1 bps mismatched ssDNA can also be detected by the developed bio-SSoC. In addition, the developed bio-SSoC also includes a SAR ADC, a microcontroller, and an OOK wireless transceiver. These built-in circuit blocks offer portable capability for applications of personal *in vitro* diagnosis (IVD). This integrated bio-SSoC is experimentally examined to have a label-free and low-concentration biomolecular detection for both Hepatitis B Virus DNA (10 fM) and cardiac troponin I protein (3.2 pM). Based on the developed bio-SSoC, both manufacturing and portability barriers can be conquered while keeping IVD in high sensitivity and selectivity. As a consequence, the momentum of mature CMOS technologies can be harnessed to promote the potential of lab-on-chip for next generation healthcare applications.

Acknowledgements

This material is based upon work supported by the National Science Council (NSC) in Taiwan (101-2220-E-002-021, 102-2220-E-002-009, and 101-2628-E-001-002-MY3) and the National Taiwan University (10R80908-1).

Notes and references

1 H. Wang, A. Silva and C.-M. Ho, *Diagnostics*, 2013, **3**, 126–154.
2 Q. Mei and Z. Zhang, *Angew. Chem., Int. Ed.*, 2012, **51**, 5602–5606.
3 S.-C. Lin, J.-C. Lu, Y.-L. Sung, C.-T. Lin and Y.-C. Tung, *Lab Chip*, 2013, **13**, 3082.
4 P. S. Waggoner and H. G. Craighead, *Lab Chip*, 2007, **7**, 1238–1255.
5 R. R. Anderson, W. Hu, J. W. Noh, W. C. Dahlquist, S. J. Ness, T. M. Gustafson, D. C. Richards, S. Kim, B. A. Mazzeo, A. T. Woolley and G. P. Nordin, *Lab Chip*, 2011, **11**, 2088–2096.
6 C.-W. Huang, H.-T. Hsueh, Y.-J. Huang, H.-H. Liao, H.-H. Tsai, Y.-Z. Juang, T.-H. Lin, S.-S. Lu and C.-T. Lin, *Sens. Actuators, B*, 2013, **181**, 867–873.
7 T.-I. Yin, Y. Zhao, J. Horak, H. Bakirci, H.-H. Liao, H.-H. Tsai, Y.-Z. Juang and G. Urban, *Lab Chip*, 2013, **13**, 834–842.
8 S. Libertino, S. Conoci, A. Scandurra and C. Spinella, *Sens. Actuators, B*, 2013, **179**, 240–251.
9 A. Hassibi and T. H. Lee, *IEEE Sens. J.*, 2006, **6**, 1380–1388.
10 Y. Cui, Q. Q. Wei, H. K. Park and C. M. Lieber, *Science*, 2001, **293**, 1289–1292.
11 G. F. Zheng, F. Patolsky, Y. Cui, W. U. Wang and C. M. Lieber, *Nat. Biotechnol.*, 2005, **23**, 1294–1301.
12 E. Stern, J. F. Klemic, D. A. Routenberg, P. N. Wyrembak, D. B. Turner-Evans, A. D. Hamilton, D. A. LaVan, T. M. Fahmy and M. A. Reed, *Nature*, 2007, **445**, 519–522.
13 C. Y. Hsiao, C. H. Lin, C. H. Hung, C. J. Su, Y. R. Lo, C. C. Lee, H. C. Lin, F. H. Ko, T. Y. Huang and Y. S. Yang, *Biosens. Bioelectron.*, 2009, **24**, 1223–1229.
14 A. Kumar, S. Aravamudhan, M. Gordic, S. Bhansali and S. S. Mohapatra, *Biosens. Bioelectron.*, 2007, **22**, 2138–2144.
15 M. K. Dawood, L. Zhou, H. Zheng, H. Cheng, G. Wan, R. Rajagopalan, H. P. Too and W. K. Choi, *Lab Chip*, 2012, **12**, 5016–5024.
16 F. Patolsky, B. P. Timko, G. H. Yu, Y. Fang, A. B. Greytak, G. F. Zheng and C. M. Lieber, *Science*, 2006, **313**, 1100–1104.
17 Y. D. Ivanov, T. O. Pleshakova, A. F. kozlov, K. A. Malsagova, N. V. Krohin, V. V. Shumyantseva, I. D. Shumov, V. P. Popov, O. V. Naumova, B. I. Fomin, D. A. Nasimov, A. L. Aseev and A. I. Archakov, *Lab Chip*, 2012, **12**, 5104–5111.

18 C.-H. Lin, C.-H. Hung, C.-Y. Hsiao, H.-C. Lin, F.-H. Ko and Y.-S. Yang, *Biosens. Bioelectron.*, 2009, **24**, 3019–3024.
19 P. R. Nair and M. A. Alam, *IEEE Trans. Electron Devices*, 2007, **54**, 3400–3408.
20 J. Li, Y. Zhang, S. To, L. You and Y. Sun, *ACS Nano*, 2011, **5**, 6661–6668.
21 J.-H. Ahn, J.-Y. Kim, K. Choi, D.-I. Moon, C.-H. Kim, M.-L. Seol, T. J. Park, S. Y. Lee and Y.-K. Choi, *IEEE Trans. Electron Devices*, 2012, **59**, 2243–2249.
22 C.-W. Huang, Y.-J. Huang, S.-S. Lu and C.-T. Lin, *Sensors*, 2012, **12**, 11592–11600.
23 S.-H. Yeh, C. Y. Tsai, J.-H. Kao, C.-J. Liu, T.-J. Kuo, M.-W. Lin, W.-L. Huang, S.-F. Lu, J. Jih, D.-S. Chen and P.-J. Chen, *J. Hepatol.*, 2004, **41**, 659–666.
24 E. Stern, A. Vacic, C. Li, F. N. Ishikawa, C. Zhou, M. A. Reed and T. M. Fahmy, *Small*, 2010, **6**, 232–238.
25 Z. Li, Y. Chen, X. Li, T. I. Kamins, K. Nauka and R. S. Williams, *Nano Lett.*, 2004, **4**, 245–247.
26 Y. L. Bunimovich, Y. S. Shin, W.-S. Yeo, M. Amori, G. Kwong and J. R. Heath, *J. Am. Chem. Soc.*, 2006, **128**, 16323–16331.
27 Z. Gao, A. Agarwal, A. D. Trigg, N. Singh, C. Fang and C. H. Tung, *et al. Anal. Chem.*, 2007, **79**, 3291–3297.
28 J. Hahm and C. M. Lieber, *Nano Lett.*, 2004, **4**, 51–54.
29 Y. Cheng, K.-S. Chen, N. L. Meyer, J. Yuan, L. S. Hirst and P. B. Chase, *et al. Biosens. Bioelectron.*, 2011, **26**, 4538–4544.
30 I. Lee, X. Luo, J. Huang, X. T. Cui and M. Yun, *Biosensors*, 2012, **2**, 205–220.
31 T. Kong, R. Su, B. Zhang, Q. Zhang and G. Cheng, *Biosens. Bioelectron.*, 2012, **34**, 267–272.
32 C. Heeschen, B. U. Goldmann, R. H. Moeller and C. W. Hamm, *Clin. Chem.*, 1998, **44**, 1925–1930.